

Supporting Information

Detailed Studies of a High-Capacity Electrode Material for Rechargeable Batteries, $\text{Li}_2\text{MnO}_3\text{-LiCo}_{1/3}\text{Ni}_{1/3}\text{Mn}_{1/3}\text{O}_2$

Naoaki Yabuuchi^a, Kazuhiro Yoshii^a, Seung-Taek Myung^b,
Izumi Nakai^a, and Shinichi Komaba^{a*}

^aDepartment of Applied Chemistry, Tokyo University of Science,
1-3 Kagurazaka, Shinjuku, Tokyo 162-8601, Japan

^bDepartment of Chemical Engineering, Iwate University, Morioka,
Iwate 020-8551, Japan

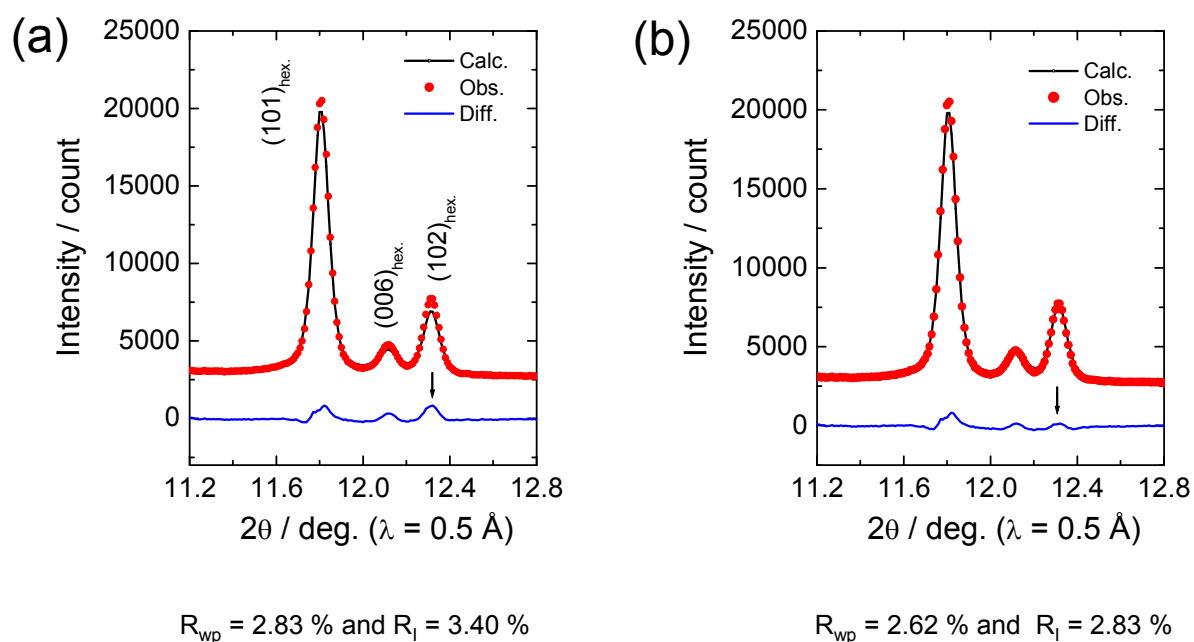


Figure S1. Highlighted SXR D patterns of the cycled $\text{Li}_x\text{Ni}_{0.13}\text{Co}_{0.13}\text{Mn}_{0.54}\text{O}_2$. Rietveld analysis was conducted using different restrictions: (a) Formation of the oxygen vacancy was not allowed in this model (occupancy of the oxygen sites was fixed), and (b) the occupancy of oxygen sites was allowed to refine. A marked difference in $(102)_{\text{hex}}$ Bragg line is observed. Refinement of the oxygen occupancy reasonably improves the reliable factors.

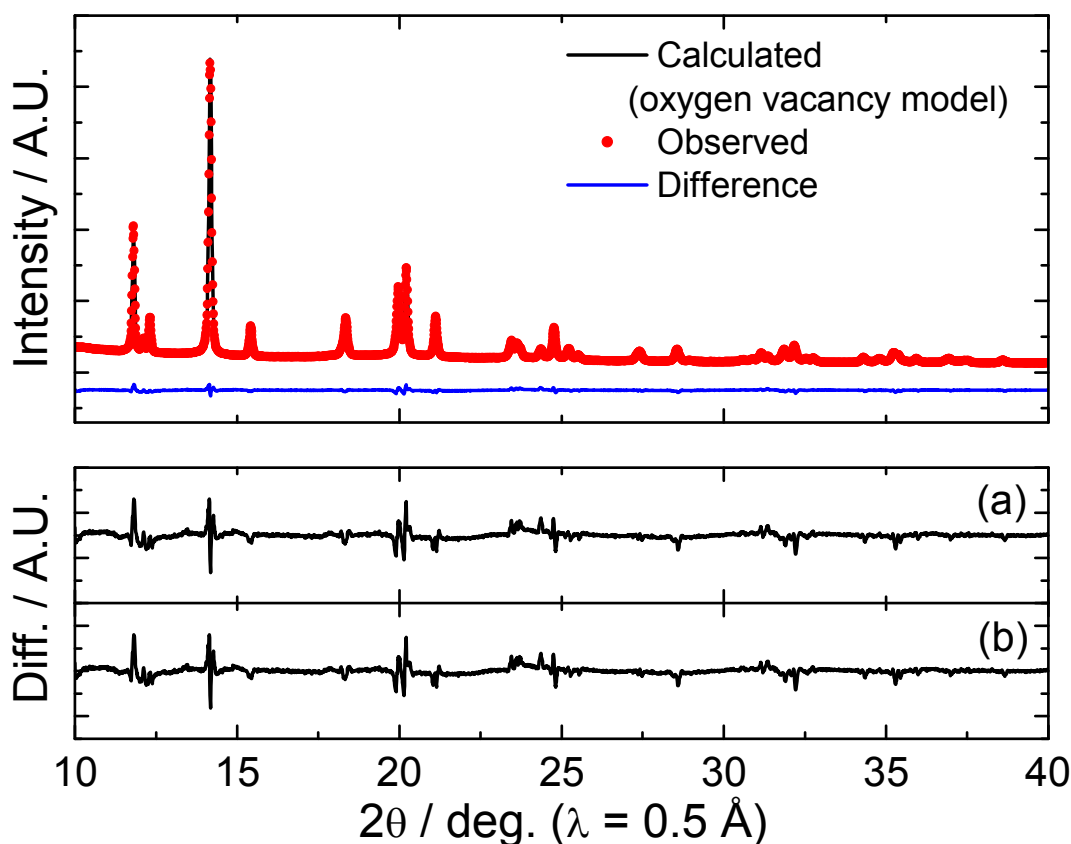


Figure S2. Comparison between the results of the Rietveld analysis on the cycled $\text{Li}_x\text{Ni}_{0.13}\text{Co}_{0.13}\text{Mn}_{0.54}\text{O}_2$ with different models; enlarged differences between observed and calculated intensity are shown with (a) oxygen vacancy model or (b) cation densification model. **In the oxygen vacancy model, total amount of Li and Me was fixed, and then the oxygen occupation and site fraction of Li and Me were refined. The refined formula was “[$\text{Li}_{0.75}\text{Me}_{0.05}\square_{0.20}$] $_{3b}$ [$\text{Li}_{0.17}\text{Me}_{0.73}\square_{0.10}$] $_{3a}$ $\text{O}_{1.85}$ ”.** In the densification model, the Li/Me ratio and oxygen occupancy were fixed, and then ratio of (Li +Me) to oxygen and site fractions were refined, leading to [$\text{Li}_{0.81}\text{Me}_{0.05}\square_{0.14}$] $_{3b}$ [$\text{Li}_{0.18}\text{Me}_{0.78}\square_{0.04}$] $_{3a}$ O_2 . Although the ratios of the lithium and metals at 3a and 3b sites are slightly different in both models, the difference observed in the XRD patterns is quite small.

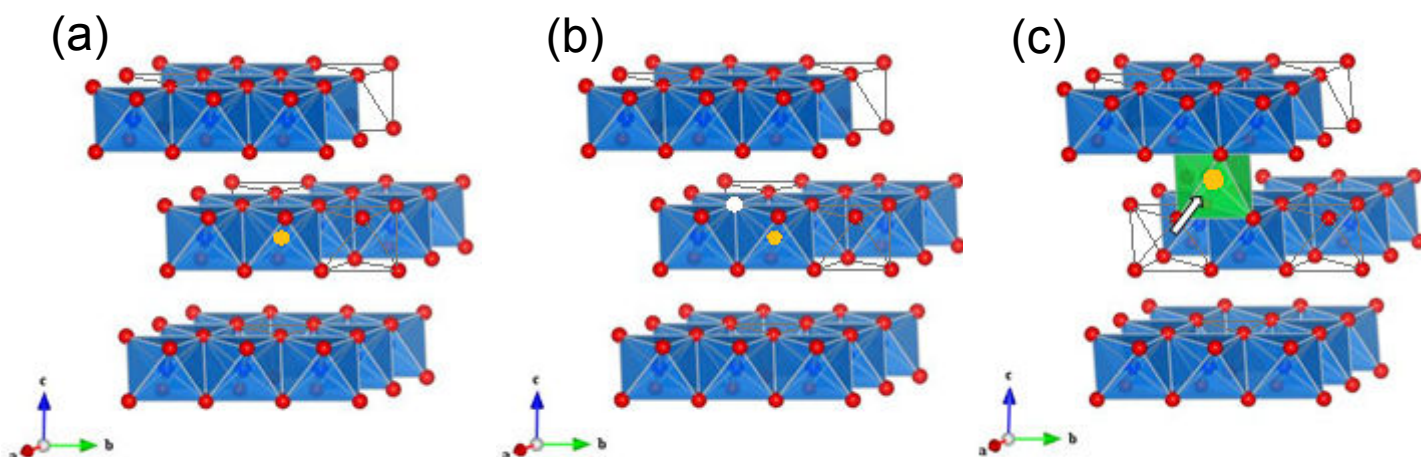


Figure S3. Schematic illustrations of the different local environments for the tetravalent nickel ions, which were used for the XANES simulation by FEFF: (a) Ni ion is located at 3a site, which is surrounded by five edge-shared 3a octahedral sites and one cation vacant site. (b) same site with (a) but one oxygen vacancy is created (denoted as a white circle in the Figure). (c) nickel ion is located at lithium 3b site, which migrated from the original octahedral 3a site. The schematics were drawn using VESTA (K. Momma and F. Izumi, *J. Appl. Crystallogr.*, 41 (2008) 653-658).

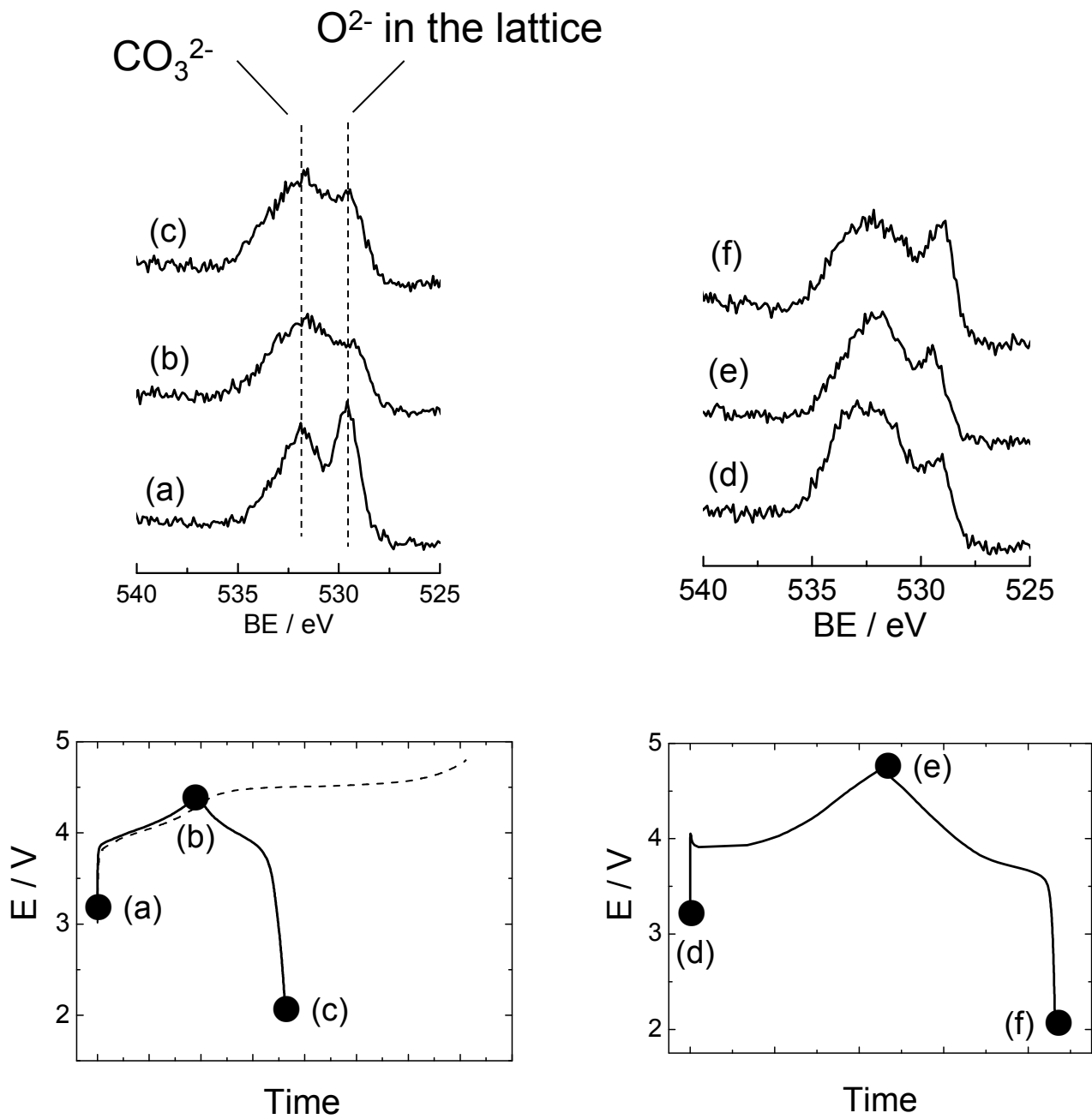


Figure S4. Oxygen 1s XPS spectra obtained from the cycled (a – c) $\text{LiNi}_{0.13}\text{Co}_{0.13}\text{Mn}_{0.54}\text{O}_2$ and (d – f) $\text{LiCo}_{1/3}\text{Ni}_{1/3}\text{Mn}_{1/3}\text{O}_2$ electrodes: (a) as-prepared ($\text{LiNi}_{0.13}\text{Co}_{0.13}\text{Mn}_{0.54}\text{O}_2$), (b) charged to 4.4 V, and then (c) discharged to 2.0 V, (d) as-prepared ($\text{LiCo}_{1/3}\text{Ni}_{1/3}\text{Mn}_{1/3}\text{O}_2$), (e) charged to 4.8 V, and then (f) discharged to the 2.0 V.

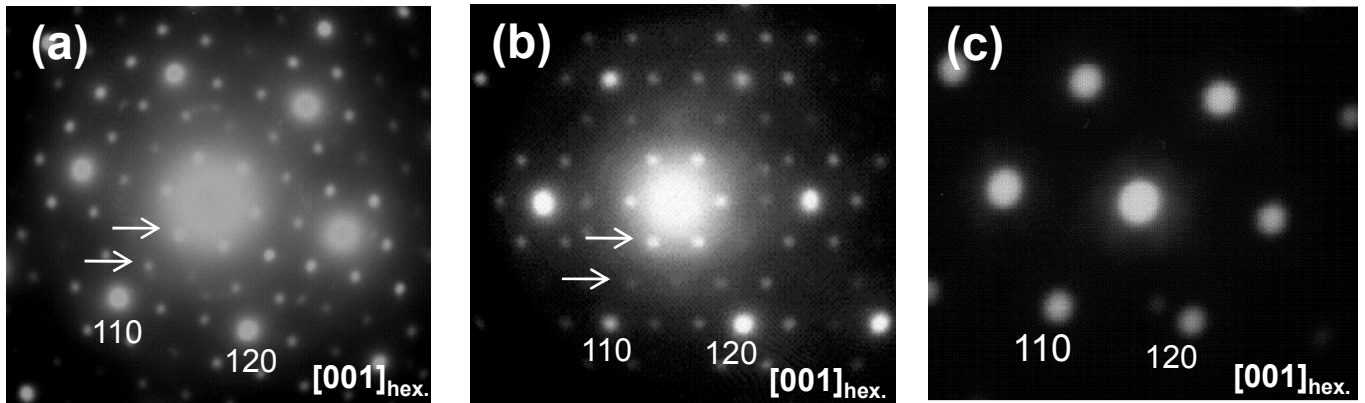


Figure S5. Electron diffraction patterns of the $\text{Li}_x\text{Ni}_{0.13}\text{Co}_{0.13}\text{Mn}_{0.54}\text{O}_{2-\delta}$ particles: (a) pristine, (b) discharged to 2.0 V after charging to (b) 4.4 V or (c) 4.8 V. Arrows indicate the tripling spots, which originated from in-plane $[\sqrt{3}a_{\text{hex.}} \times \sqrt{3}a_{\text{hex.}}]R30^\circ$ -type superlattice ordering. Note that no superlattice spots are observed after the charging to 4.8 V, suggesting that in-plane cation rearrangement process.

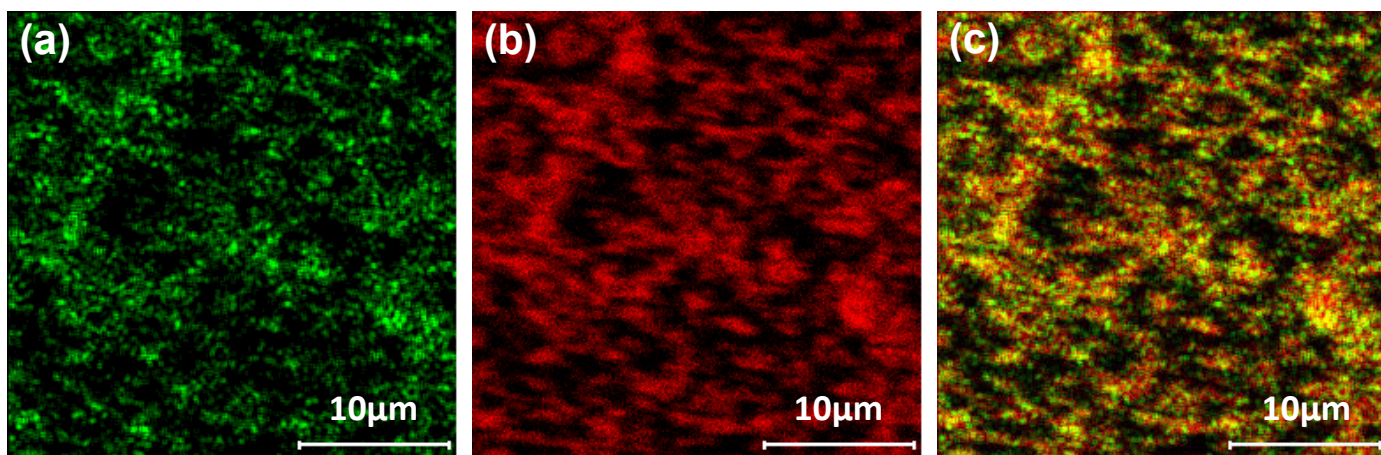


Figure S6. Two-dimensional surface map obtained by TOF-SIMS from the $\text{LiNi}_{0.13}\text{Co}_{0.13}\text{Mn}_{0.54}\text{O}_2$ electrode (as-prepared): Distribution of (a) manganese ion and (b) lithium ion in the positive-ion mode. Overlapped image between (a) and (b) is shown in (c). Li and Mn are evenly distributed throughout the as-prepared composite electrode.

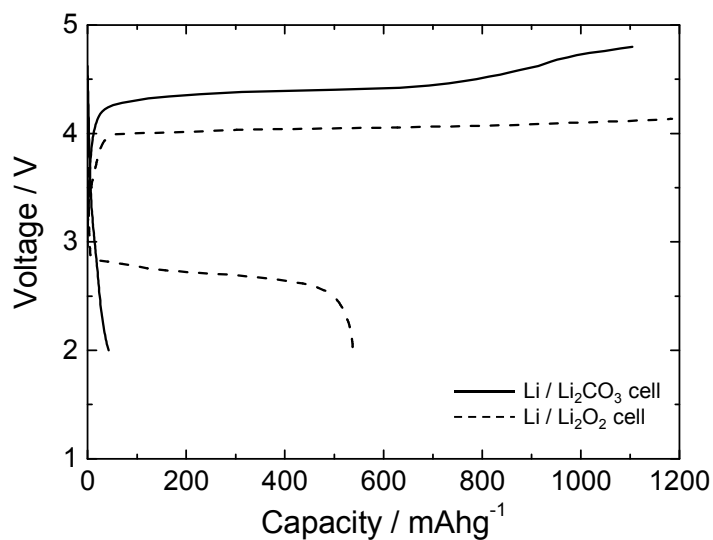


Figure S7. First charge / discharge curves of the Li / Li₂CO₃ or Li₂O₂ cells operated at a rate of 10 mA g⁻¹ at room temperature. Coin-type cells were used for the electrochemical testing. Composite electrodes consisted of 30 % Li₂CO₃ or Li₂O₂, 10 % Co₃O₄ as the catalyst, 40 % AB, and 20 % PVdF as the binder. The electrode was prepared in an Ar filled glove box without exposure to moist air.

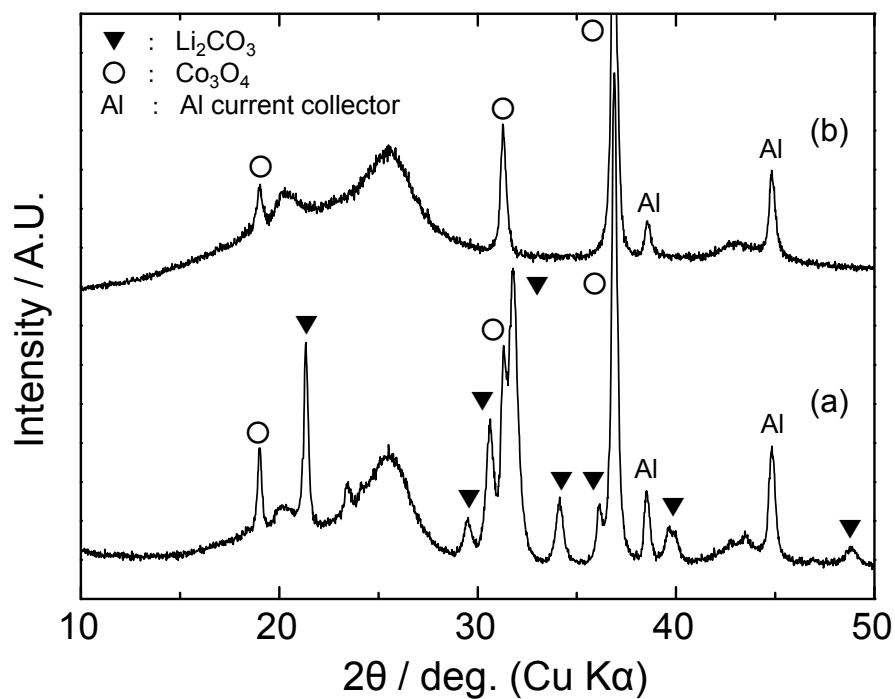


Figure S8. XRD patterns of the Li_2CO_3 composite electrodes charged at a rate of 10 mA g^{-1} at room temperature: (a) As-prepared electrode and (b) after charging to 4.8 V. The composite electrode was the same shown in Figure S7.